

Neon isotopes constrain convection and volatile origin in the Earth's mantle

Chris J. Ballentine¹, Bernard Marty^{2,3}, Barbara Sherwood Lollar⁴ & Martin Cassidy⁵

¹Department of Earth Sciences, University of Manchester, Oxford Road, Manchester M13 9LP, UK

²Centre de Recherches Pétrographiques et Géochimiques, 15 Rue Notre Dame des Pauvres, BP 20, and ³Ecole Nationale Supérieure de Géologie, Rue du Doyen Roubault, 54501 Vandoeuvre lès Nancy Cedex, France

⁴Department of Geology, University of Toronto, 22 Russell Street, Toronto, Ontario M5S 3B1, Canada

⁵Department of Geosciences, University of Houston, Houston, Texas 77204-5503, USA

Identifying the origin of primordial volatiles in the Earth's mantle provides a critical test between models that advocate magma-ocean equilibration with an early massive solar-nebula atmosphere and those that require subduction of volatiles implanted in late accreting material. Here we show that neon isotopes in the convecting mantle, resolved in magmatic CO₂ well gases, are consistent with a volatile source related to solar corpuscular irradiation of accreting material. This contrasts with recent results that indicated a solar-nebula origin for neon in mantle plume material, which is thought to be sampling the deep mantle. Neon isotope heterogeneity in different mantle sources suggests that models in which the plume source supplies the convecting mantle with its volatile inventory require revision. Although higher than accepted noble gas concentrations in the convecting mantle may reduce the need for a deep mantle volatile flux, any such flux must be dominated by the neon (and helium) isotopic signature of late accreting material.

The difference between the noble gas isotopic compositions of convecting mantle and deep mantle, sampled by mid-ocean-ridge volcanism and ocean island volcanism, respectively, has been a cornerstone of the 'layered mantle' model that has dominated our conceptual understanding of the terrestrial mantle for the past 25 years^{1,2}. The difference in the ³He/⁴He ratio between the values for plume-source basalts and the more uniform (but mostly lower) ³He/⁴He from mid-ocean-ridge basalts (MORB) was explained by a steady-state transfer of material from a primitive, volatile-rich 'lower' mantle into an 'upper' mantle, separated by the phase change at 670 km depth³. Further support for a layered mantle included the K-derived ⁴⁰Ar mass balance between the atmosphere and solid Earth, which pointed to a hidden reservoir with a ⁴⁰Ar concentration significantly higher than that in the upper mantle⁴. Similarly, the imbalance between heat and helium fluxes from the Earth was consistent with a mantle boundary layer (670 km) capable of separating these co-products of U and Th decay⁵.

Geoid and dynamic topography, seismic tomographic imaging and fluid dynamical studies, taken together, show that chemical layering is not achieved by the 670-km phase change^{6–8}. The existence of still deeper convectively isolated volatile-rich layers or regions to provide the volatile flux to the convecting mantle has been advocated^{9,10}. The compositional density contrast proposed to stabilize these regions should be observed seismically. Significantly, however, it has not been imaged¹¹. Other recent conceptual models include a water-rich melt layer within the mantle that preserves a volatile-rich deep reservoir while allowing whole-mantle convection¹². These, and the original steady-state models, source all primitive volatiles in the convecting mantle from a deep, volatile-rich reservoir.

Mantle-derived samples contain ²⁰Ne/²²Ne ratios higher than the atmospheric value (9.8), and are interpreted as evidence for trapped solar neon in the mantle². Indeed, the ²⁰Ne/²²Ne ratio of the Sun and the solar nebula is thought to be >13.4, derived from analysis of solar wind trapped in the lunar regolith (13.4–13.8), solar wind in Al foil (13.7 ± 0.3) and observation of the solar corona (13.8 ± 0.7)^{13,14}. These values are in distinct contrast to a mixture of SEP (solar energetic particle) Ne and solar-wind Ne found in meteoritic material irradiated by solar atoms and ions¹³, called

Ne-B¹⁵. The mixture of these two components is found in relatively uniform proportions to give a Ne-B value of ²⁰Ne/²²Ne = 12.5 ± 0.04 (ref. 16). Work reported in refs 16 and 17 has highlighted the importance of identifying the source of the Ne isotopes in different mantle reservoirs, as this information provides a critical evaluation of the mechanisms proposed to incorporate volatiles into the silicate Earth and, shown here, the extent of interaction between different mantle reservoirs. To date, however, interpretation has been compromised by ubiquitous air contamination found in MORB and ocean island basalt (OIB) samples¹⁸. We show in this work that magmatic natural gases can be used to obtain an unambiguous Ne isotopic value for the convecting mantle that is consistent with an irradiated meteorite origin (Ne-B). When compared to the highest reliable values found in deep mantle plume material (>13.0 ± 0.2)¹⁹, which are closer to solar nebula values, our result rules out the possibility that this OIB volatile source provides the noble gases found in the convecting mantle.

Magmatic CO₂ in New Mexico and noble gas results

Since the first identification of magmatic ³He in continental fluids, there has been an increasing awareness that magmatic CO₂ can dominate some crustal fluid systems^{20,21}. The Bravo dome natural gas CO₂ field (Fig. 1) was discovered in 1916 in Harding County, New Mexico²² (it was originally known as the Bueyeros field). Today this field is producing from over 250 wells. The gas is 98.6–99.8% CO₂ with trace amounts of N₂, CH₄ and noble gases. Earlier noble gas isotopic studies of one well in the old Bueyeros section^{23–25} show the CO₂ to be mantle-derived²³. Here, 15 samples were collected from producing wells across the field. Between 10 and 30 cm³ STP of sample gas was analysed²⁶. The ⁴He, ²⁰Ne, ⁴⁰Ar and ⁸⁴Kr abundances, and ³He/⁴He, ^{20,21}Ne/²²Ne and ⁴⁰Ar/³⁶Ar isotope ratios, were determined for each sample (Table 1). Xe isotopes, ³⁸Ar/³⁶Ar and stable isotope results will be presented in future publications.

³He/⁴He shows a coherent variation from 0.76R_a to 4.23R_a (R_a is the atmospheric ³He/⁴He = 1.4 × 10⁻⁶) across the field (Fig. 1). ²⁰Ne/²²Ne and ⁴⁰Ar/³⁶Ar show the same coherent spatial variation, and have some of the highest values measured in a free crustal fluid, up to 11.88 and 22,600, respectively. The samples define a plane in three-dimensional plots of I/²²Ne versus ²¹Ne/²²Ne versus

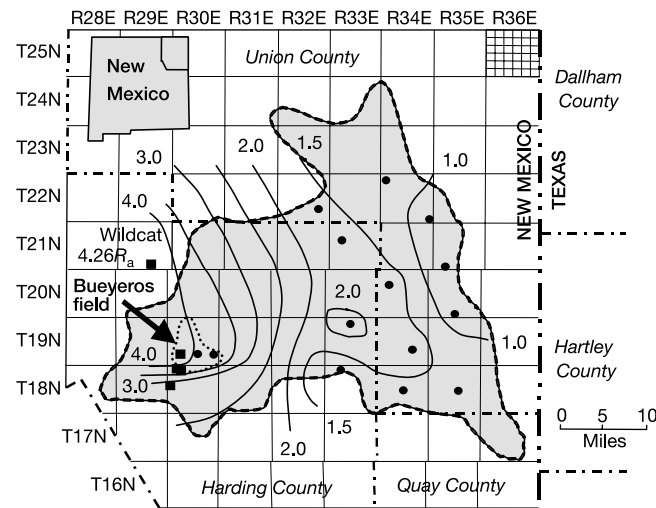


Figure 1 Study area. Filled circles, locations of samples from this study. Contours, $^3\text{He}/^4\text{He}$ ratios (expressed as R/R_a) across the field. Filled squares, locations of samples collected from non-producing wells and one wildcat well not reported here, but used in the $^3\text{He}/^4\text{He}$ contouring. The location of the historical Bueyeros field is also shown.

$^{20}\text{Ne}/^{22}\text{Ne}$ (where I is ^3He , ^4He , ^{40}Ar , ^{36}Ar or ^{84}Kr). The planes for $I = ^4\text{He}$ and ^{40}Ar are shown in Fig. 2. The equations for the best-fit planes are presented in Supplementary Information. This result shows that the same three endmembers (from crust, mantle and groundwater) can account for the noble gases in all samples.

Resolving the mantle Ne isotopic composition

Importantly, groundwater-derived (dissolved air) and crustal-derived noble gases are pre-mixed with only a small amount of variance²⁶ (Fig. 2). We show in Fig. 3a how mixing between an (air+crust) and a mantle endmember would generate a mixing wedge that defines the mantle Ne isotopic composition at its intersection with the air–MORB mixing line^{2,27}. The Bravo dome Ne isotopic data are shown in Fig. 3b, and uniquely intersect the MORB–air line at $^{20}\text{Ne}/^{22}\text{Ne} = 12.20 \pm 0.05$ and $^{21}\text{Ne}/^{22}\text{Ne} = 0.0558 \pm 0.0008$. Details of the statistical analysis of the robustness of this model and fit can be found in Supplementary Information. The identification of the mantle Ne isotopic composition by using Ne isotopes alone provides a more robust estimate than other techniques that rely *a priori* on assumed mantle isotopic or elemental abundance information. These mantle $^{20}\text{Ne}/^{22}\text{Ne}$ and

$^{21}\text{Ne}/^{22}\text{Ne}$ isotopic values can, in the simplest case, be input into the equations for the planes defined by the data, and then the mantle $I/^{22}\text{Ne}$ determined. This in turn enables the mantle $^3\text{He}/^4\text{He}$, $^{40}\text{Ar}/^{36}\text{Ar}$ and $I/^{36}\text{Ar}$ ratios also to be defined. In the Methods section, we give a more detailed discussion of the resolution of these mantle values, which are presented in Table 2.

Mantle $^3\text{He}/^4\text{He}$, $^{40}\text{Ar}/^{36}\text{Ar}$ and elemental ratios

One of the key questions regarding interpretation of the Ne isotopic result is whether or not the mantle fluids from this continental setting are representative of the convecting mantle. This issue is addressed in detail by Reid and Graham²⁸, who conclude from a Nd and He isotope study that the nearby Late Cenozoic Raton–Clayton basalts, some of which extrude over the field, are dominated by a depleted (convecting) mantle signature. Examination of the range of mantle $^3\text{He}/^4\text{He}$, $^{40}\text{Ar}/^{36}\text{Ar}$ and noble gas elemental abundance patterns (Table 2, Fig. 4) also suggest a well-gas volatile source little different to that found at mid-ocean ridges. Resolved mantle $^3\text{He}/^4\text{He}$ ratios in individual samples range from $5.4R_a$ to $7.4R_a$ (see Methods). This range is indistinguishable from $7.04 \pm 0.25R_a$ measured in local xenoliths²⁸, and is also within the average convecting mantle range of $8.75 \pm 2.14R_a$. The resolved well-gas mantle $^{40}\text{Ar}/^{36}\text{Ar}$ of between 37,000 to 55,200 is significantly higher than the value of 25,000 estimated from bulk analysis of the volatile-rich basalt glass IID43 ‘popping rock’ used as a reference sample for many noble gas models of the mantle system²⁷. However, variability of $^{40}\text{Ar}/^{36}\text{Ar}$ in bulk basalt glass samples can occur even for the same $^{20}\text{Ne}/^{22}\text{Ne}$ value¹⁶, and is probably related to atmospheric contamination of whole-rock analyses¹⁸. Laser decrepitation of individual fluid inclusions in the popping-rock sample record values of up to $^{40}\text{Ar}/^{36}\text{Ar} = 64,000 \pm 15,000$ (ref. 29). Studies of other MORB samples report values as high as $42,400 \pm 9,700$ (ref. 30). The question has been raised as to whether even the highest observed values are subject to contamination²⁹. Well-gas samples are not subject to the same mechanism of air contamination as basalt glasses, and are corrected for the air component (see Methods). The resolved range of mantle $^{40}\text{Ar}/^{36}\text{Ar}$ in the well gases therefore confirms the highest measured values, and defines (to our knowledge, for the first time) the $^{40}\text{Ar}/^{36}\text{Ar}$ limit for the convecting mantle (Table 2).

Confirmation of the high mantle $^{40}\text{Ar}/^{36}\text{Ar}$ has an important consequence. Bulk analysis popping-rock data are used to determine the convecting mantle noble gas abundance pattern, which is normalized to ^{36}Ar . On the basis of the results of this study, the mantle ^{36}Ar from the popping-rock whole-rock analyses has been overestimated by a factor of up to ~ 2 , and is clearly subject to some degree of air contamination. Whereas this correction can be made

Table 1 Noble gas results

Sample	$^3\text{He}/^4\text{He}$ (R/R_a)	Error	$^{20}\text{Ne}/^{22}\text{Ne}$	Error	$^{21}\text{Ne}/^{22}\text{Ne}$	Error	$^{40}\text{Ar}/^{36}\text{Ar}$	Error	^4He (10^{-5})	Error (10^{-6})	^{20}Ne (10^{-9})	Error (10^{-11})	^{40}Ar (10^{-5})	Error (10^{-7})	^{84}Kr (10^{-10})	Error (10^{-12})
BD01	1.670	0.008	10.664	0.034	0.05623	0.00031	10,723	393	9.44	1.1	1.69	1.7	3.03	2.9	1.01	3.6
BD02	0.764	0.004	9.955	0.035	0.05006	0.00032	4,660	59	41.5	5.0	7.00	7.1	6.52	5.9	5.04	13
BD03	0.896	0.004	10.014	0.012	0.05152	0.00014	5,346	92	33.1	4.0	5.21	4.7	5.36	4.2	3.24	8.0
BD04	1.611	0.008	10.585	0.043	0.05409	0.00035	9,911	237	9.61	1.1	1.81	1.9	2.86	2.4	1.03	2.5
BD05	0.965	0.005	9.930	0.014	0.05255	0.00024	5,412	56	27.0	3.3	4.46	4.0	5.38	4.2	3.33	7.4
BD06	1.503	0.008	10.488	0.038	0.05612	0.00043	9,213	206	12.0	1.4	2.02	2.0	3.50	2.8	1.35	3.1
BD07	2.104	0.011	11.201	0.049	0.05416	0.00041	10,955	387	7.81	0.95	1.80	2.1	2.80	2.5	0.900	3.5
BD08	1.143	0.006	10.214	0.027	0.05778	0.00037	6,650	90	16.1	1.9	2.64	2.5	3.96	3.3	2.00	4.7
BD09	1.724	0.009	10.735	0.051	0.05779	0.00054	ND	ND	9.80	1.2	1.80	2.1	ND	ND	ND	ND
BD10	1.104	0.006	10.196	0.021	0.05371	0.00029	6,726	106	19.9	2.4	3.08	2.9	3.96	3.0	2.02	4.3
BD11	3.784	0.019	11.880	0.047	0.05647	0.00044	21,560	1,591	3.91	0.47	1.03	1.3	2.41	3.5	0.455	1.8
BD12	3.627	0.018	ND	ND	ND	ND	21,019	1,279	4.15	0.50	ND	ND	2.42	2.9	0.467	2.3
BD12 _{repeat}	3.634	0.018	11.603	0.061	0.05373	0.00024	22,612	3,061	4.13	0.50	1.20	1.5	2.40	3.8	0.490	2.3
BD13	1.318	0.007	10.250	0.046	0.05792	0.00045	7,735	277	15.3	1.8	2.40	2.8	3.82	3.8	1.92	4.9
BD14	1.413	0.007	10.543	0.125	0.05825	0.00023	8,517	645	11.5	1.4	1.79	3.2	3.07	2.7	1.23	3.3
WB2	4.070	0.022	11.617	0.178	0.05583	0.00139	21,452	460	3.76	0.282	1.09	2.4	ND	ND	0.404	11
Bueyeros (ref. 24)	3.136	0.321	11.6	0.9	0.062	0.008	16,200	340	1.67	6.30	9.86	9.8	3.3	9.8	0.435	0.41

All values corrected for full procedural blanks equivalent to $(5 \pm 2) \times 10^{-9} \text{ cm}^3 \text{ STP } ^4\text{He}$, $(5 \pm 2) \times 10^{-11} \text{ cm}^3 \text{ STP } ^{20}\text{Ne}$, $(6 \pm 2) \times 10^{-8} \text{ cm}^3 \text{ STP } ^{40}\text{Ar}$, $(1.4 \pm 0.52) \times 10^{-11} \text{ cm}^3 \text{ STP } ^{84}\text{Kr}$. Blank Ne and Ar isotopic ratios are atmospheric, while the blank $^3\text{He}/^4\text{He} = (1.397 \pm 0.007)R_a$. Concentrations in $\text{cm}^3 \text{ STP cm}^{-3}$. Errors are 1σ . ND, not determined.

with confidence to $\text{He}/^{36}\text{Ar}$ and $\text{Ne}/^{36}\text{Ar}$ ratios, the mechanism of air addition to basalt glasses remains poorly understood¹⁸, and the possibility that air Kr and Xe contamination has occurred in the basalt glass reference sample cannot be discounted. The mantle noble gas abundance pattern derived from well gases, with the air component unambiguously removed, therefore provides a new and critical data resource (Table 2), and is little different to the new $^{36}\text{Ar}_{\text{air}}$ -corrected popping rock (Fig. 4) (also see Supplementary Information).

The origin of resolved $^{20}\text{Ne}/^{22}\text{Ne}$

There are four possible reasons why the resolved $^{20}\text{Ne}/^{22}\text{Ne}$ of the well gases is lower than the solar value of 13.8: (1) enhanced ^{22}Ne nucleogenic production in the mantle is reducing a ratio that was originally solar; (2) solar-air mixing; (3) enrichment in the heavier isotopes of a reservoir residual from a mass-fractionating process such as diffusion; or (4) a trapped component (Ne-B) in accreting material^{16,17} is dominating the Ne inventory of the mantle source. To generate a mantle $^{20}\text{Ne}/^{22}\text{Ne} = 12.2$ – 12.5 and $^{21}\text{Ne}/^{22}\text{Ne} = 0.0558$ from solar values by nucleogenic production requires a mantle $^{21}\text{Ne}/^{22}\text{Ne}$ production ratio of 0.28, some 166 times lower than the predicted value^{2,31}. Crustal gas values are lower than those predicted for an homogeneous system by a factor of 5–7 because of preferential U + Th siting with the dominant ^{22}Ne -producing target element (fluorine)³¹. However, in the mantle only about one-third of the nucleogenic ^{22}Ne is produced by α -particle interaction with fluorine, requiring this route to be enhanced by a factor of ~ 500 (ref. 2). Element siting effects are unlikely to be able to account for the difference (more than two orders of magnitude) required.

Reduction of solar $^{20}\text{Ne}/^{22}\text{Ne} = 13.8$ to 12.5 by air-recycling into the mantle requires a 30% air Ne ($^{20}\text{Ne}/^{22}\text{Ne} = 9.8$) addition. We do not envisage any process that could introduce an elementally unfractionated air component into the mantle. Most systems, including sediments³² and water, are variably enriched in heavy noble gases relative to modern air. If we take deep sea water as an example, a 30% air Ne addition to the mantle would result in 310%,

220% and 130% of the Ar, Kr and Xe respectively in the popping rock being air-derived. It is shown above that because of air contamination Kr and Xe are overestimated in the popping-rock sample, and this estimate then represents a minimum. It follows that the addition of air-Ne with appropriate heavy noble gas enrichment would result in mantle $^{38}\text{Ar}/^{36}\text{Ar}$, Kr and Xe isotopic compositions dominated by air. $^{129}\text{Xe}/^{130}\text{Xe}$ ratios in excess of the air value found in both MORB popping rock³³ and Bravo dome well gas^{23–25} eliminates this possibility.

Preferential loss of lighter isotopes to reduce the $^{20}\text{Ne}/^{22}\text{Ne}$ from 13.8 to 12.5 by mass-dependent diffusion can be modelled as a simple reduced-mass Rayleigh fractionation. This would require an 80% loss of ^{22}Ne from an originally solar mantle reservoir. The same loss would reduce the pre-deuterium burning $^3\text{He}/^{22}\text{Ne}$ ratio from a solar value of 1.5 to 0.5. This is in the wrong direction to produce the resolved $^3\text{He}/^{22}\text{Ne} = 2.6$ – 2.8 in the well gas, which are minimum values in the case of phase fractionation effects during magmatic degassing (see Supplementary Information). At $^{20}\text{Ne}/^{22}\text{Ne} = 12.5$, $^3\text{He}/^{22}\text{Ne}$ in popping rock is even higher at 4.9 (Table 2), requiring an initial mantle $^3\text{He}/^{22}\text{Ne}$ of 15, an order of magnitude greater than the solar nebula value. Similar arguments apply when considering the similarity of the resolved mantle $^{84}\text{Kr}/^{22}\text{Ne}$ ratio in both popping rock and well gases (Table 2). We discount mass-dependent fractionation.

The value of the convecting mantle resolved in this study is indistinguishable from the Ne-B component found in solar-wind-irradiated meteoritic material. It would be fortuitous if the convecting mantle had evolved a Ne isotopic composition by either ancient (pre- ^{129}I , ^{244}Pu decay) air-addition or nucleogenic production to this same value, and we have ruled out the most viable processes that could do this from their predicted effect on the other noble gases. The most probable explanation for low $^{20}\text{Ne}/^{22}\text{Ne}$ in the well-gas mantle source is that it originated as a trapped component (Ne-B) implanted by solar corpuscular irradiation of accreting material^{16,17}. To preserve this value, subsequent atmosphere recycling, nucleogenic or other non-Ne-B neon admixtures to the mantle must have been minimal.

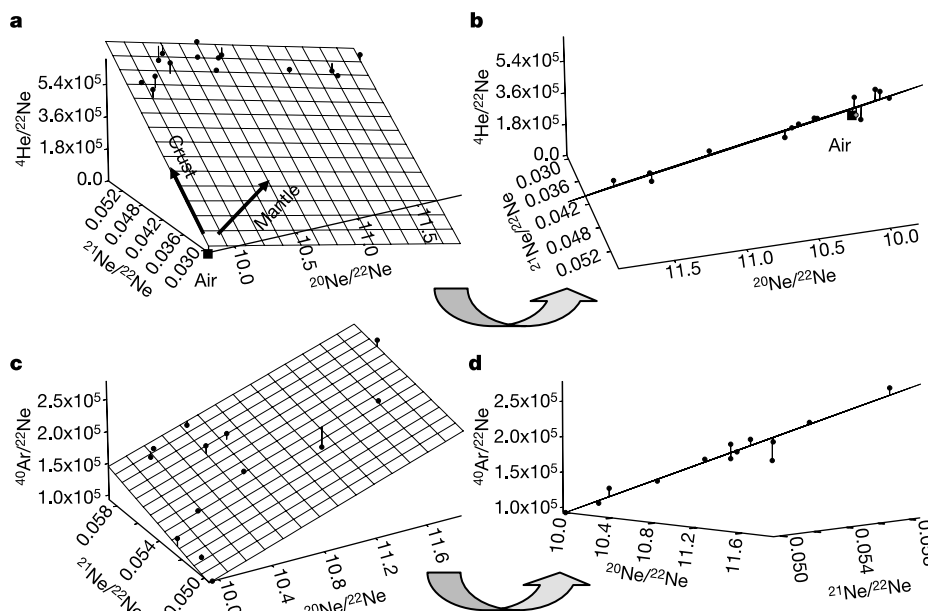


Figure 2 Correlation of measured $^{21}\text{Ne}/^{22}\text{Ne}$, $^{20}\text{Ne}/^{22}\text{Ne}$ with $^4\text{He}/^{22}\text{Ne}$ and $^{40}\text{Ar}/^{22}\text{Ne}$. **a, c**, Planes of best fit; **b, d**, rotations of the graph to view the plane edge-on. **a**, The small variance in the crust+air component suggests that the air- and crustal-derived noble gases are premixed in the groundwater system²⁶ before variable interaction with the

magmatic fluid. **c**, The $^{40}\text{Ar}/^{22}\text{Ne}$ fit to a plane again passes close to the air endmember (not shown). **b, d**, The good fit to a plane shows that the elemental abundance and isotopic data can be described by the same three endmember components for all samples.

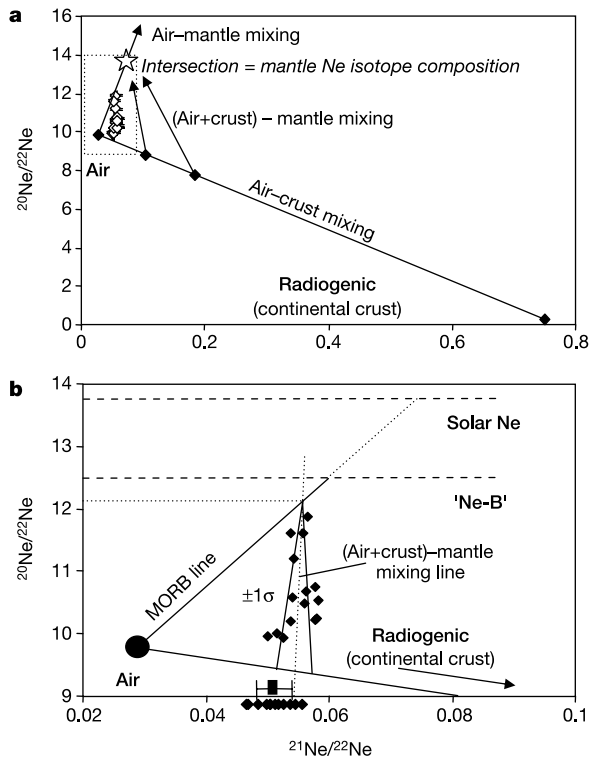


Figure 3 Intersection of a two-component air+crust mixture with the MORB air–mantle mixing line defines the mantle Ne isotopic endmember. **a**, Diagram showing different possible mixing lines. **b**, Bravo dome data projected onto the $^{20}\text{Ne}/^{22}\text{Ne}$ versus $^{21}\text{Ne}/^{22}\text{Ne}$ plane, showing a pseudo-two-component mix between air+crust and mantle components. The scatter from a single mixing line is because of a small amount of variance in the air+crust mixing ratio. The average and 1σ variance of the resolved air+crust component (see Supplementary Information) is shown on the x axis. The data intersect the MORB air–mantle line^{2,27} at $^{20}\text{Ne}/^{22}\text{Ne} = 12.20 \pm 0.05$.

Convection models and the origin of volatiles in the mantle

MORB has higher and distinct $^3\text{He}/^{22}\text{Ne}$ compared with Hawaii³⁴, Iceland^{35–37} or Kola¹⁹. Fluxing models therefore need to have different residence times for He and Ne in the convecting mantle. This could be caused by differential extraction at mid-ocean ridges. Alternatively, preferential transferral of He relative to Ne from the proposed volatile-rich source needs to be invoked by this form of model. Although these processes cannot be simply ruled out, they provide an additional level of complexity when justifying the flux models. The observation that the Iceland plume source has a $^{20}\text{Ne}/^{22}\text{Ne}$ ratio indistinguishable from solar (13.75 ± 0.32 ; ref. 37) contrasts markedly with the Ne isotopic ratio of the mantle source resolved in this work. Although the Iceland measurement is the subject of debate^{16,18}, more recent data from the Kola peninsula reports reproducible plume source $^{20}\text{Ne}/^{22}\text{Ne} > 13.0 \pm 0.2$ (ref. 19). This is again consistent with a solar rather than a Ne-B

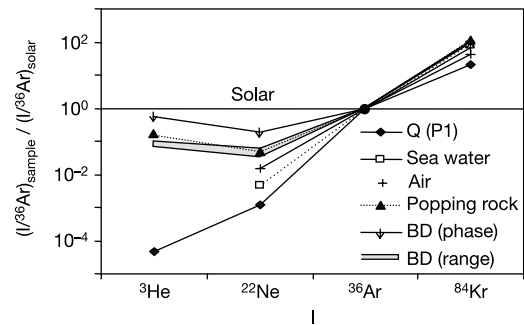


Figure 4 Mantle noble gas isotopes relative to ^{36}Ar normalized to the solar abundance, relative to ^{36}Ar (Table 2). The range of values derived from the Bush dome study is shown as a shaded area, BD (range), and compared with the popping-rock sample, corrected for the original literature ^{36}Ar overestimate (see text). With the exception of a small ^3He deficit in the well-gas system, the elemental abundance pattern of popping rock and the well gases are indistinguishable. Also shown is the limit estimated for phase fractionation of the magmatic gases, BD (phase) (see Supplementary Information), air, sea water and the Q (P1) trapped component in primitive meteorites⁵⁰.

origin for Ne in the plume source.

An average noble gas concentration in the convecting mantle that is higher by a factor of ~ 3.5 would remove the need for either a ^3He flux into the convecting mantle or a hidden ^{40}Ar -rich reservoir, and the heat–helium imbalance could then be accounted for by temporal variance in the ocean-ridge helium flux within a whole-mantle convective regime³⁸. This has been called the ‘zero paradox’ model concentration. This would allow the decoupling of the plume and convecting-mantle volatile systems suggested by the $^3\text{He}/^{22}\text{Ne}$ and Ne isotopic difference highlighted here. But recent constraints^{39–41} on average convecting mantle Nb/ CO_2 , $\text{CO}_2/^3\text{He}$ and Nb make it unlikely that the ‘zero paradox’ ^3He concentration is reached. Uncertainty within these values means that the ^3He concentration may nevertheless be higher than that used by current flux models, reducing the noble gas flux required from a deep mantle source. As there is no obvious process capable of reducing a solar Ne isotopic ratio to the Ne isotopic value observed in the well gases, the source of the Kola and perhaps the Icelandic plume material cannot provide the noble gases in the convecting mantle. We therefore argue that any solar Ne heterogeneity is only a small component of a Ne-B dominated deep mantle source.

The neon isotope heterogeneity of the mantle also has profound implications for the processes and timing of Earth accretion. A significant fraction of terrestrial accretion took place when the solar nebula was still present in the first 10 Myr of the accretionary process. During this period, planetary bodies the size of Mars formed and differentiated, indicated independently by dynamical simulations⁴² and the extinct radioactivity systematics of SNC meteorites and other differentiated bodies^{43–45}. Thus, solar-nebula gas could have been trapped directly during accretion and compaction, or indirectly during magmatic episodes and equilibration with

Table 2 Resolved mantle elemental and isotopic ratios

	$^3\text{He}/^4\text{He}$	$^{20}\text{Ne}/^{22}\text{Ne}$	$^{40}\text{Ar}/^{36}\text{Ar}$	$^4\text{He}/^{21}\text{Ne}^*$	$^3\text{He}/^{22}\text{Ne}$	$^4\text{He}/^{40}\text{Ar}$	$^3\text{He}/^{36}\text{Ar}$	$^{22}\text{Ne}/^{36}\text{Ar}$	$^{84}\text{Kr}/^{36}\text{Ar}$
Bravo dome	$7.05R_a$	12.5	55,200	1.23×10^7	2.56	1.09	0.50	0.1953	0.0545
Bravo dome	$5.35R_a$	12.2	37,000	1.45×10^7	2.77	0.844	0.33	0.1202	0.0482
Popping rock†	$8.3R_a$	12.5	25,000–44,000*	1.68×10^7	4.90	$1.06^* - 1.52$	0.40 (0.8)§	0.0816 (0.163)§	0.0284 (0.0568)§
Air	–	9.8	295.5	–	–	–	–	0.0530	0.0207
Sea water	–	9.8	295.5	–	–	–	–	0.0156	0.0405
Solar	–	13.8	–	–	$1.5\ddagger$	–	$5.1\ddagger$	3.4	5.05×10^{-4}

$^{21}\text{Ne}^*$ indicates mantle ^{21}Ne corrected for solar contribution².

* Ref. 29.

† Ref. 27.

‡ Pre-deuterium burning, see ref. 19.

§ Corrected for ^{36}Ar overestimate (see text).

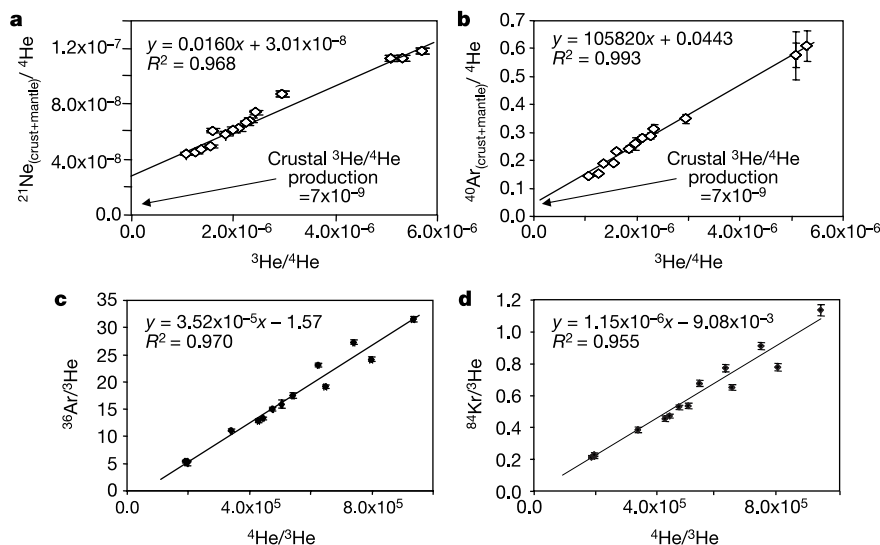


Figure 5 Resolving endmember compositions from simple mixing. Elemental ratios plotted against $^3\text{He}/^4\text{He}$ (**a**, **b**) or $^4\text{He}/^3\text{He}$ (**c**, **d**) are used to derive crustal and mantle endmember values (see Methods and Table 2). Air-corrected ^{21}Ne (using mantle $^{20}\text{Ne}/^{22}\text{Ne} = 12.5$) (**a**) and air-corrected ^{40}Ar (**b**) are normalized to ^4He to generate true

mantle–crust two-component mixing lines. Measured $^{36}\text{Ar}/^3\text{He}$ (**c**) and $^{84}\text{Kr}/^3\text{He}$ (**d**) versus $^4\text{He}/^3\text{He}$ define pseudo-two-component mixing lines between crust+air and mantle endmembers. All y -axis error bars are 1σ confidence. Errors in $^3\text{He}/^4\text{He}$ (Table 1) or $^4\text{He}/^3\text{He}$ are within the plotted symbol.

massive early planetary atmospheres⁴⁶. It has also been shown that under such circumstances a significant amount of noble gases could be partitioned into core-forming phases⁴⁷. Gas loss processes could also occur, for example, during collision with large impactors⁴⁶. In the case of the solid Earth, extensive volatile loss up to 80 Myr after accretion is shown by the relative proportions of the Xe daughter products of extinct ^{129}I and ^{244}Pu (ref. 2). Late infall of solar-corpiscular-irradiated material could then form a significant volatile source for the degassed planetary bodies, with entrainment into the mantle possible in an early, dry subducting system⁴⁸. The occurrence of solar-nebula gases in plumes is then evidence of either a remnant of the silicate mantle that preserves an accretionary volatile history distinct from that of the convecting mantle, or a portion of the mantle that has received its different volatile composition as a result of interaction with the core. The D'' density contrast with the convecting mantle may have helped to preserve the distinct character of this portion of the mantle over time⁴⁸. The results presented here, however, suggest that the bulk of the terrestrial silicate mantle He and Ne is dominated by solar-corpiscular-irradiated accretionary material. □

Methods

Resolving the mantle noble gas components

Resolution of the isotopic and elemental characteristics of the mantle noble gases depends first on the resolved mantle $^{20}\text{Ne}/^{22}\text{Ne}$ and $^{21}\text{Ne}/^{22}\text{Ne}$ values. A magmatic fluid interacting with a fluid at a near-constant air+crust mixing ratio defines a unique (air+crust)–mantle mixing wedge (Fig. 3). The intersection of the data wedge with the air–MORB line at $^{20}\text{Ne}/^{22}\text{Ne} = 12.20 \pm 0.05$ is, however, lower than the accepted Ne-B value of 12.5. As we discuss, there are few viable mechanisms to reduce the $^{20}\text{Ne}/^{22}\text{Ne}$ ratio from solar to lower values, and we must consider the possibility that the choice of the air–MORB line may introduce some uncertainty. We therefore consider $^{20}\text{Ne}/^{22}\text{Ne}$ mantle values along the mixing line up to 12.5 (Fig. 3), providing a sensitivity test for the resolved mantle components. Although input of the mantle Ne isotopic values into the equations for the respective equations for a plane provides the simplest conceptual method of determining the relationship between Ne and the other mantle-derived noble gases, care must be taken with this approach as the plane fits are neither error-weighted nor have an error assessment of the extrapolated values. We show here how the Ne isotopes are used to allow a full error assessment of resolved components.

Crustal noble gas isotopic production ratios, like those in air, are well defined³¹. The mantle-, air- and crustal-Ne isotope endmembers then define the proportion of these components in each individual sample⁴⁹ (Supplementary Tables 1 and 2), where, for example:

$$^{21}\text{Ne}_{\text{total}} = ^{21}\text{Ne}_{\text{air}} + ^{21}\text{Ne}_{\text{crust}} + ^{21}\text{Ne}_{\text{mantle}} \quad (1)$$

Resolved $^{21}\text{Ne}_{\text{air}}$ is subtracted from $^{21}\text{Ne}_{\text{total}}$ to leave ‘air-corrected’ ^{21}Ne , $^{21}\text{Ne}_{(\text{crust+mantle})}$. A plot of $^{21}\text{Ne}_{(\text{crust+mantle})}/^4\text{He}$ against $^3\text{He}/^4\text{He}$, with a negligible air-helium component, then develops a simple two-component mixing line (Fig. 5a). Extrapolation to the crustal $^3\text{He}/^4\text{He}$ endmember value ($^3\text{He}/^4\text{He}_{\text{crust}} = 0.007R_a$)³¹ defines the local $^4\text{He}/^{21}\text{Ne}$ crustal input value, $^4\text{He}/^{21}\text{Ne}_{\text{crust}}$, to be between $(3.47 \pm 0.24) \times 10^7$ and $(3.30 \pm 0.23) \times 10^7$ for $^{20}\text{Ne}/^{22}\text{Ne} = 12.2$ and 12.5 (Fig. 5a), respectively. These values are indistinguishable, and illustrate the insensitivity of the resolved crustal components to the choice of the mantle Ne isotopic endmember value.

The crustal ^3He and ^4He contribution to each sample can then be calculated from $^{21}\text{Ne}_{\text{crust}}$, $^3\text{He}/^4\text{He}_{\text{crust}}$ and $^4\text{He}/^{21}\text{Ne}_{\text{crust}}$. This crustal ^3He and ^4He component can be subtracted from the observed crust/mantle helium mixture to determine the mantle $^3\text{He}/^4\text{He}$ endmember for each sample. Three samples give a mantle component $^3\text{He}/^4\text{He}$ determination with propagated errors of $<50\%$. For $^{20}\text{Ne}/^{22}\text{Ne} = 12.2$ and 12.5, samples BD07, BD11 and BD12 give crust-corrected $^3\text{He}/^4\text{He}$ values of $5.18 \pm 0.76R_a$ to $7.42 \pm 1.61R_a$, $5.29 \pm 0.42R_a$ to $7.11 \pm 0.77R_a$, and $5.58 \pm 0.52R_a$ to $7.69 \pm 1.00R_a$, with an error-weighted average of $5.35 \pm 0.36R_a$ to $7.4 \pm 0.5R_a$, for the magmatic $^3\text{He}/^4\text{He}$ endmember. These compare with 4.9–6.0 R_a , derived from the full data set defined planes (Supplementary Information). Extrapolation of the $^{21}\text{Ne}_{(\text{crust+mantle})}/^4\text{He}$ mixing line to mantle $^3\text{He}/^4\text{He}$ values defines the range of $^{21}\text{Ne}/^4\text{He}_{\text{mantle}}$ values resolved by this data set.

Crustal and mantle $^{40}\text{Ar}/^{36}\text{Ar}$ ratios are both large, 6.1×10^7 (ref. 31) and $>2.5 \times 10^5$ respectively, compared with the air ratio. This allows ^{40}Ar in excess of $^{40}\text{Ar}_{\text{air}}$, $^{40}\text{Ar}_{(\text{crust+mantle})}$ to be calculated, where:

$$^{40}\text{Ar}_{(\text{crust+mantle})} = ^{40}\text{Ar}_{\text{total}} [1 - (^{40}\text{Ar}/^{36}\text{Ar})_{\text{air}} / (^{40}\text{Ar}/^{36}\text{Ar})_{\text{sample}}] \quad (2)$$

$^{40}\text{Ar}_{(\text{crust+mantle})}/^4\text{He}$ plotted against $^3\text{He}/^4\text{He}$ then also generates a simple two-component mixing line (Fig. 5b). Extrapolation to the mantle $^3\text{He}/^4\text{He}$ values gives the range of resolved $^{40}\text{Ar}/^4\text{He}_{\text{mantle}}$ ratios.

$^{36}\text{Ar}_{\text{total}}$ and $^{84}\text{Kr}_{\text{total}}$ are treated as two-component mixtures of crust+air and mantle. Although there is some variance in the crust+air mixing ratio (Fig. 2), plots of $^{36}\text{Ar}_{\text{total}}/^3\text{He}$ and $^{84}\text{Kr}_{\text{total}}/^3\text{He}$ versus $^4\text{He}/^3\text{He}$ produce pseudo-two-component mixing lines that converge towards the mantle $^4\text{He}/^3\text{He}$ (Fig. 5c, d). The convergence of data and high correlation coefficients provide confidence in this approach. Extrapolation to the mantle $^4\text{He}/^3\text{He}$ values then gives the range of $^{36}\text{Ar}/^3\text{He}_{\text{mantle}}$ and $^{84}\text{Kr}/^3\text{He}_{\text{mantle}}$ respectively. Combining the mantle $^3\text{He}/^4\text{He}$ with $^{21}\text{Ne}/^4\text{He}_{\text{mantle}}$, $^{40}\text{Ar}/^4\text{He}_{\text{mantle}}$, $^{36}\text{Ar}/^3\text{He}_{\text{mantle}}$ and $^{84}\text{Kr}/^3\text{He}_{\text{mantle}}$ provides the range of isotopic and elemental abundance ratios presented in Table 2.

Received 9 July; accepted 4 November 2004; doi:10.1038/nature03182.

- Allège, C. J., Staudacher, T., Sarda, P. & Kurz, M. Constraints on evolution of Earth’s mantle from rare gas systematics. *Nature* **303**, 762–766 (1983).
- Porcelli, D. & Ballentine, C. J. Models for the distribution of terrestrial noble gases and evolution of the atmosphere. *Rev. Min. Geochem.* **47**, 411–480 (2002).
- Porcelli, D. & Wasserburg, G. J. Mass transfer of helium, neon, argon, and xenon through a steady-state upper mantle. *Geochim. Cosmochim. Acta* **59**, 4921–4937 (1995).
- Hart, R., Dymond, J. & Hogan, L. Preferential formation of the atmosphere-sialic crust system from the upper mantle. *Nature* **278**, 156–159 (1979).
- O’Nions, R. K. & Oxburgh, E. R. Heat and helium in the Earth. *Nature* **306**, 429–431 (1983).
- Davies, G. F. & Richards, M. A. Mantle convection. *J. Geol.* **100**, 151–206 (1992).
- Van der Hilst, R. D., Widiyantoro, S. & Engdahl, E. R. Evidence for deep mantle circulation from

- global tomography. *Nature* **386**, 578–584 (1997).
8. Van Keken, P. E. & Ballentine, C. J. Dynamical models of mantle volatile evolution and the role of phase transitions and temperature-dependent rheology. *J. Geophys. Res.* **B 104**, 7137–7151 (1999).
 9. Kellogg, L. H., Hager, B. H. & Van der Hilst, R. D. Compositional stratification in the deep mantle. *Science* **283**, 1881–1884 (1999).
 10. Becker, T. W., Kellogg, J. B. & O'Connell, R. J. Thermal constraints on the survival of primitive blobs in the lower mantle. *Earth Planet. Sci. Lett.* **171**, 351–365 (1999).
 11. Vidale, J. E., Schubert, G. & Earle, P. S. Unsuccessful initial search for a midmantle chemical boundary with seismic arrays. *Geophys. Res. Lett.* **28**, 859–862 (2001).
 12. Bercovici, D. & Karato, S. Whole-mantle convection and the transition-zone water filter. *Nature* **425**, 39–44 (2003).
 13. Wieler, R. Noble gases in the solar system. *Rev. Min. Geochem.* **47**, 21–70 (2002).
 14. Kallenbach, R. *et al.* Isotopic composition of solar wind neon measured by CELIAS/MTOF on board SOHO. *J. Geophys. Res.* **A 102**, 26895–26904 (1997).
 15. Black, D. C. On the origin of trapped helium, neon, and argon isotopic variations in meteorites — I Gas-rich meteorites, lunar soil and breccia. *Geochim. Cosmochim. Acta* **36**, 347–375 (1972).
 16. Trieloff, M., Kunz, J., Clague, D. A., Harrison, D. & Allègre, C. J. The nature of pristine noble gases in mantle plumes. *Science* **288**, 1036–1038 (2000).
 17. Trieloff, M., Kunz, J. & Allègre, C. J. Noble gas systematics of the Réunion mantle plume source and the origin of primordial noble gases in Earth's mantle. *Earth Planet. Sci. Lett.* **200**, 297–313 (2002).
 18. Ballentine, C. J., Porcelli, D. & Wieler, R. Technical comment on 'Noble gases in mantle plumes' by Trieloff *et al.* (2000) and reply. *Science* **291**, 2269, doi:10.1126/science.291.5512.2269a (2001).
 19. Yokochi, R. & Marty, B. A determination of the neon isotopic composition of the deep mantle. *Earth Planet. Sci. Lett.* **225**, 77–88 (2004).
 20. Sherwood Lollar, B., Ballentine, C. J. & O'Nions, R. K. The fate of mantle-derived carbon in a continental sedimentary basin: Integration of C/He relationships and stable isotope signatures. *Geochim. Cosmochim. Acta* **61**, 2295–2307 (1997).
 21. Ballentine, C. J., Schoell, M., Coleman, D. & Cain, B. A. 300-Myr-old magmatic CO₂ in natural gas reservoirs of the west Texas Permian basin. *Nature* **409**, 327–331 (2001).
 22. Broadhead, R. F. Carbon dioxide in northeast New Mexico. *West Tex. Geol. Soc. Bull.* **32**, 5–8 (1993).
 23. Staudacher, T. Upper mantle origin for Harding County well gases. *Nature* **325**, 605–607 (1987).
 24. Phinney, D., Tennyson, J. & Frick, U. Xenon in CO₂ well gas revisited. *J. Geophys. Res.* **B 83**, 2313–2319 (1978).
 25. Caffee, M. W. *et al.* Primordial noble gases from Earth's mantle: Identification of a primitive volatile component. *Science* **285**, 2115–2118 (1999).
 26. Ballentine, C. J. & Sherwood Lollar, B. Regional groundwater focusing of nitrogen and noble gases into the Hugoton-Panhandle giant gas field, USA. *Geochim. Cosmochim. Acta* **66**, 2483–2497 (2002).
 27. Moreira, M., Kunz, J. & Allègre, C. J. Rare gas systematics in popping rock: isotopic and elemental compositions in the upper mantle. *Science* **279**, 1178–1181 (1998).
 28. Reid, M. R. & Graham, D. W. Resolving lithospheric and sub-lithospheric contributions to helium isotope variations in basalts from the southwestern US. *Earth Planet. Sci. Lett.* **144**, 213–222 (1996).
 29. Burnard, P., Graham, D. & Turner, G. Vesicle specific noble gas analyses of popping rock: Implications for primordial noble gases in Earth. *Science* **276**, 568–571 (1997).
 30. Marty, B. & Humbert, F. Nitrogen and argon isotopes in oceanic basalts. *Earth Planet. Sci. Lett.* **152**, 101–112 (1997).
 31. Ballentine, C. J. & Burnard, P. G. Production, release and transport of noble gases in the continental crust. *Rev. Min. Geochem.* **47**, 481–538 (2002).
 32. Torgersen, T. & Kennedy, B. M. Air-Xe enrichments in Elk Hills oil field gases: role of water in migration and storage. *Earth Planet. Sci. Lett.* **167**, 239–253 (1999).
 33. Kunz, J., Staudacher, T. & Allègre, C. J. Plutonium-fission xenon found in Earth's mantle. *Science* **280**, 877–880 (1998).
 34. Honda, M. & McDougall, I. Primordial helium and neon in the Earth—a speculation on early degassing. *Geophys. Res. Lett.* **25**, 1951–1954 (1998).
 35. Dixon, E. T., Honda, M., McDougall, I., Campbell, I. H. & Sigurdsson, I. Preservation of near-solar neon isotopic ratios in Icelandic basalts. *Earth Planet. Sci. Lett.* **180**, 309–324 (2000).
 36. Moreira, M., Breddam, K., Curtice, J. & Kurz, M. D. Solar neon in the Icelandic mantle: new evidence for an undegassed lower mantle. *Earth Planet. Sci. Lett.* **185**, 15–23 (2001).
 37. Harrison, D., Burnard, P. & Turner, G. Noble gas behaviour and composition in the mantle: constraints from the Iceland Plume. *Earth Planet. Sci. Lett.* **171**, 199–207 (1999).
 38. Ballentine, C. J., van Keken, P. E., Porcelli, D. & Hauri, E. H. Numerical models, geochemistry and the zero paradox noble-gas mantle. *Phil. Trans. R. Soc. Lond. A* **360**, 2611–2631 (2002).
 39. Saal, E. S., Hauri, E. H., Langmuir, C. H. & Perfit, M. R. Vapour undersaturation in primitive mid-ocean-ridge basalt and the volatile content of Earth's upper mantle. *Nature* **419**, 451–455 (2002).
 40. Marty, B. & Tolstikhin, I. N. CO₂ fluxes from mid-ocean ridges, arcs and plumes. *Chem. Geol.* **145**, 233–248 (1998).
 41. Su, Y. & Langmuir, C. H. *Global MORB Chemistry Compilation at the Segment Scale* (Department of Earth and Environmental Sciences, Columbia University, 2003; available at (<http://petdb.ldeo.columbia.edu/documentation/morbcompilation/>)).
 42. Wetherill, G. W. in *Origin of the Moon* (eds Hartmann, W. K., Phillips, R. J. & Taylor, G. J.) 519–555 (Oxford Univ. Press, Oxford, 1986).
 43. Halliday, A. N., Wänke, H., Birck, J. L. & Clayton, R. N. The accretion, composition and early differentiation of Mars. *Space Sci. Rev.* **96**, 1–34 (2001).
 44. Yin, Q. Z. *et al.* A short timescale for terrestrial planet formation from Hf-W chronometry of meteorites. *Nature* **418**, 949–952 (2002).
 45. Kleine, T., Munker, C., Mezger, K. & Palme, H. Rapid accretion and early core formation on asteroids and the terrestrial planets from Hf-W chronometry. *Nature* **418**, 952–955 (2002).
 46. Porcelli, D., Woolum, D. S. & Cassen, P. Deep Earth rare gases: initial inventories, capture from the solar nebula, and losses during Moon formation. *Earth Planet. Sci. Lett.* **193**, 237–251 (2001).
 47. Porcelli, D. & Halliday, A. N. The core as a possible source of mantle helium. *Earth Planet. Sci. Lett.* **192**, 45–56 (2001).
 48. Tolstikhin, I. & Hofmann, A. W. Early crust on top of the Earth's core. *Phys. Earth Planet. Inter.* (in the press).
 49. Ballentine, C. J. & O'Nions, R. K. The nature of mantle neon contributions to Vienna Basin hydrocarbon reservoirs. *Earth Planet. Sci. Lett.* **113**, 553–567 (1992).
 50. Ott, U. Noble gases in meteorites—trapped components. *Rev. Min. Geochem.* **47**, 71–100 (2002).

Supplementary Information accompanies the paper on www.nature.com/nature.

Acknowledgements Access and permission to sample was by permission of BP (the field is now owned by Oxy) and the Bravo dome field manager, D. Holcomb. Sampling from the West Bush dome was by permission of Amerada Hess. H. Baur provided laboratory support. We thank F. Albarède, D. Porcelli, A. Halliday, A. Hofmann, C. Hall, J. Gilmour, G. Holland, D. Murphy, R. Yokochi and I. Tolstikhin for discussions and critical comments that have improved this Article. This work was funded by the Zurich ETH and NERC.

Competing interests statement The authors declare that they have no competing financial interests.

Correspondence and requests for materials should be addressed to C.J.B. (chris.ballentine@manchester.ac.uk).